

Reflectivity enhancement through appropriate sized gold particles for optical coherence tomography in functional imaging applications

Uma Maheswari Rajagopalan^{1,*}, Shunsuke Uematsu², Hirofumi Kadono² and Manabu Tanifuji³

¹*SIT Research Lab., Shibaura Institute of Technology, Tokyo, Japan*

²*Graduate School of Science and Engineering, Saitama University, Shimo-Okubo 251, Urawa, Saitama 338-0825, Japan*

³*RIKEN Brain Science Institute, 2-1 Hirosawa, Wako-city, Saitama, 351-0198, Japan Hirosawa, Saitama Ken, 351-0198 Japan*

This article is dedicated to Prof T Asakura

We propose a method for enhancing the reflectivity of optical coherence tomography (OCT) signals through introduction of gold nano particles into the sample under study. The radius of the gold nano particles that gives maximum backscattering at an illuminating wavelength and a certain index of the medium can be determined based on Mie scattering theory. We have demonstrated our proposal by phantom experiments done with gold particles suspended in agarose mixed with intra-lipid. We could clearly see an enhancement in OCT reflectivity by a factor of 4 at a wavelength of 1310 nm and for a gold nano particle of radius 125 nm. © Anita Publications. All rights reserved.

Keywords: Optical coherence tomography, Scattering, gold nano particles, reflectivity, enhancement, Mie scattering

1 Introduction

Optical coherence tomography (OCT) has been widely and routinely used for ophthalmological applications as well as getting popular in various other fields [1-4]. In applications of OCT including deep structure such as brain imaging that is supposed to be a highly scattering tissue, it becomes essential to enhance the reflectivity as much as possible to improve signal to noise ratio. One such potential application with deep structure brain imaging is functional OCT or monitoring dynamical changes that we introduced as functional OCT (fOCT) in our group for brain and retinal imaging [5-7]. fOCT is a technique of monitoring changes in the OCT reflectivity signal following the application of a stimulus for example activation of a living brain with a odor stimulus or a visual stimulus and application of chemical in the case of a plant and so on. Due to the possibility of acquisition of images in 3D as well as performing deep tissue imaging, there are many groups working toward investigating the potential of fOCT [8-11].

In fOCT, we define a differential signal or a change in the reflectivity of the OCT signal. This differential signal is the averaged reflectivity signal measured from the biological system, in our case, living brain responding to a visual stimulus against an averaged reflectivity signal obtained under no visual stimulus condition. As the differential signals are very small, we propose a method of enhancing the reflectivity by introducing gold particles as contrast agents. Gold particles have been commonly used now as immunogold specific labels and various sized particles are easily available. Based on Mie theory, for a chosen wavelength, by making a proper choice of the size of the scattering particle in relation to the index of the surrounding medium, it can be shown that the back scattering efficiency can be greatly enhanced.

Corresponding author :

e-mail: uma@shibaura-it.ac.jp; (Uma Maheswari Rajagopalan)

*This work was done when Rajagopalan U. M was working at RIKEN, Japan

In this paper, first with gold particles as scattering particles and the surrounding medium being the intra-lipid suspended in agarose, we first theoretically estimated the appropriate radius of the particle using Mie theory. Next, we did basic scattering experiments to confirm the enhancement of back-scattered intensity by varying the radius of the gold particle. Finally, we made a phantom of layered structure that contained a layer of proper sized particle and conducted OCT to demonstrate that indeed back-scattering efficiency of the OCT reflectivity can be enhanced.

2 Theoretical background

Here, we restrict the discussion on Mie scattering to a very minimal as it can be found in a few well written text books [12-15]. Whenever a plane wave is incident upon a particle having a discrete boundary that has different refractive index from its surroundings, a scattered wave is generated. Mie theory provides an exact solution for the scattered field by such a spherical particle and the scattered field is characterized by the size parameter m_a and refractive index mismatch n_r , where

$$m_a = 2\pi a / (\lambda/n_{\text{med}})$$

and

$$n_r = n_p/n_{\text{med}}$$

with λ being the wavelength of the illuminating light, a being the radius of the particle, n_p index of the particle and n_{med} the index of the surrounding medium. The scattering efficiency is defined as

$$Q_{\text{sca}} = C_{\text{sca}}/A$$

with C_{sca} being the scattering cross-section calculated analytically for a spherical particle from Mie calculation and A being the geometrical cross section.

Further, the scattering particles are generally characterized by a parameter called reduced scattering coefficient defined as $\mu_s' = \mu_s(1-g)$. Here μ_s is the scattering coefficient and given as $NQ_{\text{sca}}A$ with N being the number of scattering particles. g gives the probability for scattering along a particular direction θ . For g taking a value of 0, the scattering is isotropic. When g is positive, forward scattering dominates and when g is negative, there will be more backward scattering.

Therefore, in order to increase the backscattering, there are two ways that can be done:

1. To increase the scattering coefficient μ_s ,
2. To have the g value close to zero.

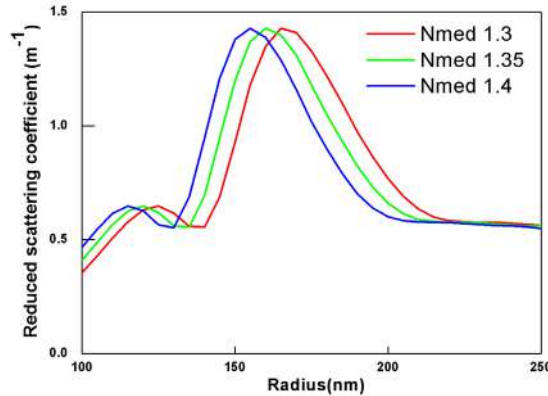


Fig 1. Variation of the reduced scattering coefficient plotted as a function of the particle radius under three different refractive indices of the medium. Depending on the index of the medium, there exists a suitable radius of the particle that gives the highest scattering cross-section.

Figure 1 shows reduced scattering cross-section μ_s' calculated analytically as a function of the particle radius under three different medium indices that are approximately close to the index of tissue samples assuming a g -value of 0. As can be seen, depending on the value of the index of the surrounding medium, μ_s' differs. This fact can be advantageously used in increasing the scattering cross-section by making an appropriate choice of the particle in relation to the refractive index of the medium.

In case of biological medium, index of the medium is not known exactly. In the actual case, biological medium consists of different organelles with individual differences in the index values and having sizes almost the size of λ or less. In such cases, the scattering is anisotropic with forward scattering being dominant and very little being back scattered. So, by having a contrast agent that makes the scattering anisotropy of the medium toward isotropic, we can basically increase the overall back scattering efficiency of the medium. This is the basic idea behind the enhancement of the signal. As gold particles are generally used in labeling of biological specimens, we started off our phantom experiments with gold particles. We did first Monte Carlo simulation to confirm the basic results of OCT reflectivity enhancement [16].

3 Experiments and results

In order to demonstrate the proposal of enhancement of back scattering, we conducted some basic scattering experiments with different sizes of scattering particles. Here the particles have been chosen to be spherical due to the easy availability.

3.1. Fundamental scattering characteristics

Figure 2 shows the schematic of the experimental system used for measuring the scattered light. Light from a laser diode operating at a visible wavelength of 635.9 nm was focused onto a sample speculum plate that consisted of a slide glass and a cover glass. The light scattered from the sample was measured by a photodiode mounted on a rotating stage. Phase sensitive detection was done with a lock-in amplifier by modulating the light from LD through modulating the driving current with a waveform of 1 kHz from the internal oscillator of the lock-in amplifier. Sample consisted of polystyrene particles suspended in water filling the gap of the speculum plate. The thickness of the plate was set to be 0.07 mm. With respect to the direction of propagation z , the transmitted light direction is considered as 0° . The scattered light was measured at every $\pm 10^\circ$ with the positive sign indicating anti-clockwise direction while the negative sign indicating clockwise direction of the scattered light. Figure 3 shows the scattering characteristic of polystyrene particles of different radii namely 53.5 nm, 240 nm and 526.5 nm which respectively correspond to the size parameters of 0.53, 2.37 and 5.20.

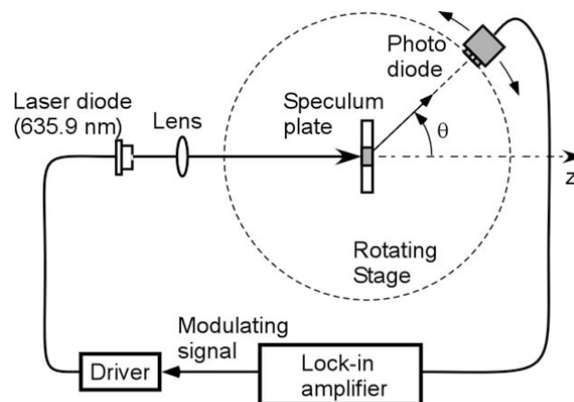


Fig 2. A basic schematic of the experimental system used for demonstrating scattering characteristics. Here the photodiode was mounted on a rotating stage to measure the scattered intensity from different scattering angles.

As can be seen from Fig 3, for the case of the size factor of 0.53, for both forward and backward directions, scattering is mainly characterized by Rayleigh. Usual convention is that when the size of the particle is ten times smaller than the wavelength used, the scattering characteristic follows Rayleigh with the scattered intensity following λ^{-4} variation. While for the other two cases of the polystyrene spheres, the scattering is mainly characterized by strong forward and a rather weak backward scattering. These results that agree with the Mie scattering calculations confirm the validity of the current system in measurement of scattering properties.

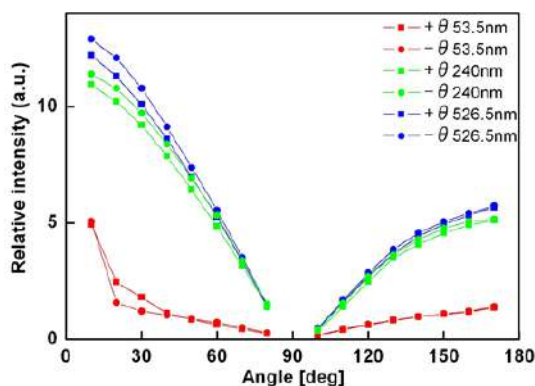


Fig 3. Results of scattered intensity given as a function of the scattering angle for three different polystyrene particles with size factors namely, 0.53, 2.37 and 5.2 suspended in water.

Next, we used the same system to evaluate the scattering characteristics of gold colloidal particles. From Mie calculations, for a wavelength of 639.5 nm, the appropriate radius of the gold particle giving maximum backscattered intensity with the medium index being 1.4 is 75 nm. So, we chose three different kinds of particles having radii of 40 nm, 75 nm and 125 nm. The concentrations correspond to 0.01% and the gap of the speculum plate was set to be 1 mm. As compared to the case of polystyrene spheres where the gap was only 0.07 mm, for gold particles we need to increase the gap almost 14 times so as to increase the backscattered light intensity. This is due to the fact that the specular reflection is strong with almost no deeper propagation.

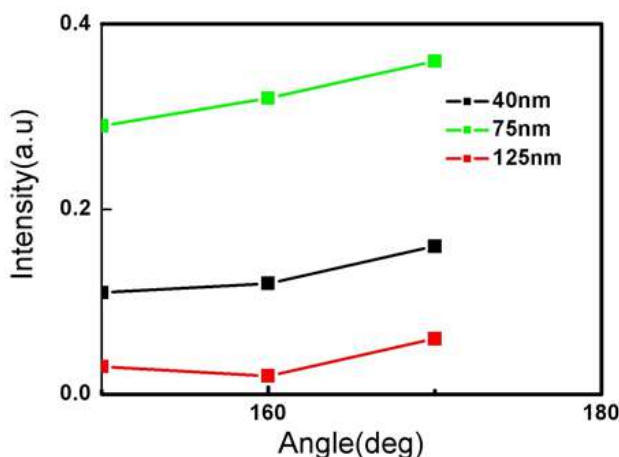


Fig 4. Backscattered intensity from gold colloidal particles suspended in water for three different radii of the particle namely, 40nm, 75nm and 125nm obtained under the wavelength of the light being 635.9 nm given as a function of the backscattering scattering angle.

Figure 4 shows the backscattered light from different angles of 150° to 170° . In order to measure the scattering enhancement of the particles, initially, background intensity without the gold suspension was measured. Relative intensity was calculated as an increase in the scattered intensity after subtracting out the background intensity. The results of the variation of backscattered intensities from gold nanoparticles suspended in water are shown as a function of the backscattering angle for different radii of the particles. The different radii of 40 nm, 75 nm and 125 nm, respectively correspond to black, green and red lines. Here, we chose the size of the particles that were close to the required optimum size based on their availability in the market. As can be seen from the Fig 4, with increasing backscattering angle, the backscattered intensity increases for all three types of particles. These results agree with the basic Mie-scattering calculations.

We summarize the results of gold particles suspended in water in Table 1. The value obtained for the gold particles having a radius of 75 nm is maximum. This value of radius is close to the optimal radius under the wavelength of 635.9 nm and at a refractive index of the surrounding medium being 1.4. The backscattered intensity from the gold nanoparticles of the optimal radius of 75 nm is almost 2.3 times larger than that of gold nanoparticles of radius of 125 nm. So there is a clear indication about the effect of the size of the appropriate choice of the particle radius with respect to the wavelength used and index of the surrounding medium in enhancing the backscattered light intensity.

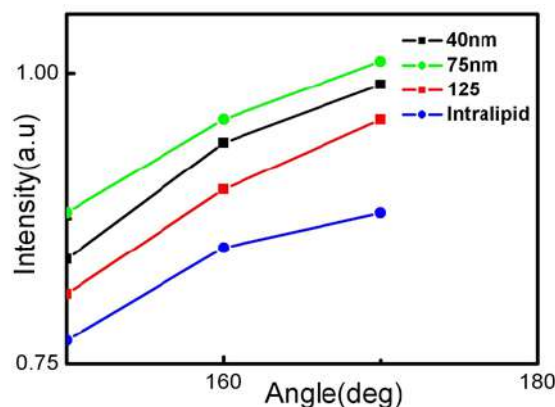


Fig 5. Variation of the backscattered intensity given as function of backscattering angle from gold colloidal particles suspended in intralipid. Here, the intralipid was used to generate the equivalent tissue scattering condition. The wavelength of light was 635.9 nm and the particle radii 40 nm (black), 75 nm (green) and 125 nm (red) were shown in different colours. Blue line corresponds to the intralipid only without any gold colloidal particles.

In order to have a sample that has scattering characteristics close to a tissue medium, we used intralipid as suspension medium for the gold particles and measured the backscattered intensities. A suspension ratio of 6:4 was used for the intralipid and gold colloid that would finally give a concentration of 0.004% gold particles. The concentration of intralipid used was 10%.

Figure 5 shows the backscattered intensity as a function of the back scattering angle for gold particles of three different sizes suspended in intralipid and water. Again the backscattered light intensity increases with respect to backscattering angle and the increase is the largest for particles of 75 nm radius. Again, referring to the Table 1, which summarizes the variation of the backscattered intensities for different particle types and radii, we can see that there is a decrease in the enhancement of the backscattered intensity for the particles suspended in intralipid in comparison to the enhancement of the backscattered intensity for the particles suspended in water. The increase with respect to lipid is around 15% for particles of 75 nm radii, while for 40 nm and 125 nm, the values correspond to 13% and 9%, respectively. The small enhancement

is considered to be due to the very low concentration of 0.004% of gold particles compared to the previous case of 0.01%. Further, due to the use of intralipid, there seems to be some clustering for example for 40 nm case, the enhancement is almost close to the 70 nm case. Here, the use of intralipid as a scattering medium is necessary for the reasons listed below:

1. The specular reflection is very strong that makes difficult to detect the effect of gold particles.
2. We want to prepare the phantoms close to the biological tissue. The scattering characteristics of intralipid is close to that of the biological tissue and due to this property, the intralipid is generally used in making tissue phantoms with predefined scattering characteristics and thus in simulation of biological tissue.

3.2 OCT experiment with phantoms

A schematic of the time-domain OCT experimental system to demonstrate the OCT reflectivity signal enhancement is shown in Fig 6. The system consists of a Mach-Zehnder type heterodyne interferometer built from single mode fibers. The source is a broadband source and it operates at a central wavelength of 1310 nm and has a bandwidth of 50 nm. The estimated depth resolution in air of the system with a mirror sample is 34 μm . Light from the source was split into two beams with a optical coupler having a splitting ratio of 19:1 into sample (19 parts) and reference beam (1 part). Both sample and reference beams were modulated by acousto-optic modulators (AOM1 and AOM2) to shift the optical frequencies by 116 and 116.25 MHz, respectively. AOMS are used to perform phase-sensitive detection. Polarization controllers PC1 and PC2 were used to optimize the plane of polarization illuminating the AOM1 and AOM2 while PC3 and PC4 were used to maximize the interference amplitude. Light reflected from the sample and the mirror was combined with a coupler 2, respectively at a coupling ratio of 19:1 to produce the interference signal which was then detected by the detector.

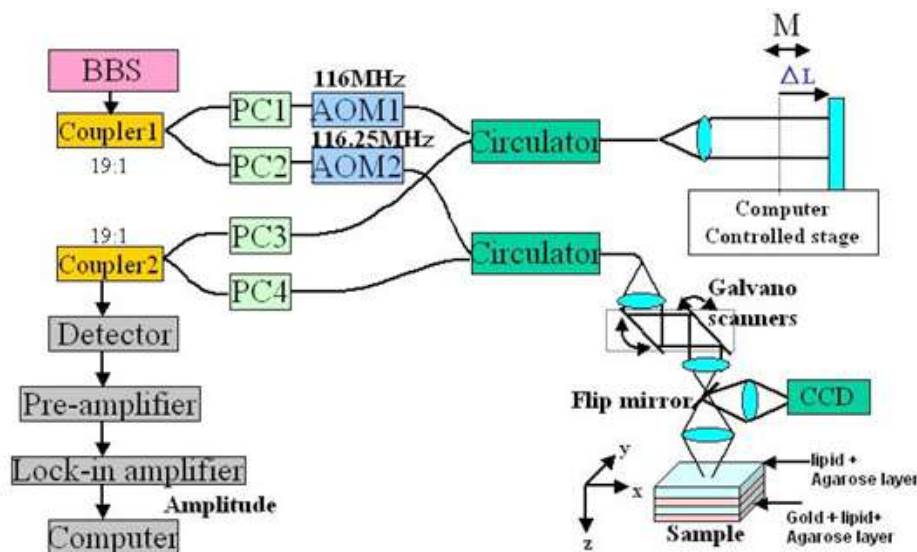


Fig 6. A schematic of the time domain OCT system to measure the OCT reflectivity with a sample phantom consisting of 4 layers. The phantom sample consisted of four alternate layers of agarose in lipid followed by colloidal gold particles in lipid and agarose, respectively indicated in blue and pink colors.

Reflected beams from the reference mirror and the sample could only interfere when the total path length difference is within the coherence length of the source. So by moving the reference mirror and changing the reference plane, it is possible to optically slice the sample or in other words get reflected light from an arbitrary plane of the sample. The reference mirror was mounted on a mechanical stage and scanned

at a speed of 2 mm/sec through a motion controller. On the sample side, we have a probe unit installed with galvano mirrors so as to perform surface scans. Probe unit is fitted with an objective lens of NA 0.1 giving a beam diameter of 16 μm . Probe unit is also fitted with a CCD camera so as to fix the point of interest on the sample.

In order to simulate the biological tissue, we first designed a phantom consisting of 4 layers. A schematic of the phantom is shown in the inset of Fig 6. The total thickness of the phantom is 0.8 mm with the layer 1 being 0.2 mm. First and third layers contain only agarose in lipid while the second and fourth layers contain agarose in lipid with gold colloidal particles. We made three different phantoms by varying the radius of the gold colloidal particles to namely 40 nm, 75 nm and 125 nm. Concentration of the agarose in lipid was set to be 1.2%. Therefore, our results based on Mie scattering calculated for an operating wavelength of 1310 nm and assuming a putative value of 1.4 for the index of the surrounding medium, the theoretical value for obtaining the strongest or the maximum backscattered intensity is 160nm.

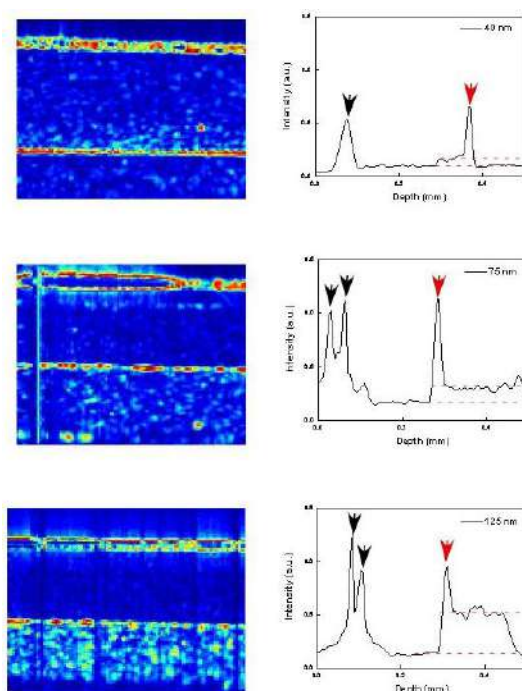


Fig 7. Results of enhancement in OCT reflectivity obtained with phantom layered structure containing gold colloidal nanoparticles of radii 40 nm (top), 75nm (middle) and 125 nm (bottom). Here the left column shows the OCT x-z images with red corresponding to the strong back scattering or high OCT reflectivity region and blue corresponding to low OCT reflectivity region. The right column shows the averaged OCT reflectivity profiles as a function of z with averaging done across x. Black and red arrows respectively indicate the peaks corresponding to the respective interfaces, air-agarose+lipid interface and air- agarose+lipid+gold within the phantom. Red dashed lines indicate the base corresponding to the background used in calculating the enhancement ratio due to the presence of gold colloidal particles.

Figure 7 shows the results obtained with the left column showing the x-z scan image of the phantom sample for 40 nm, 75 nm and 125 nm and the right column giving the corresponding intensity variation. In the left column OCT x-z images, red corresponds to the strong back scattering or high OCT reflectivity region and blue corresponding to low OCT reflectivity region. The right column shows the averaged OCT reflectivity profiles as a function of z with averaging done across x. Red dashed lines indicate the base corresponding to

the background used in calculating the enhancement ratio due to the addition of gold colloidal particles. The enhancement ratio was obtained as a ratio of the peak height to the background of the base of the reflectivity signal. In order to estimate the background, the mean of a few nearest pixels around the peak pixel was calculated was defined as the background level. The ratio of the peak to the background level was used as the enhancement ratio and the ratio was compared for the two different conditions of agarose + lipid and agarose+ lipid + colloidal gold particles under different sizes of the colloidal particles.

Table 1. A table of maximum backscattered intensities measured at 635.9 nm (middle column) for particles suspended of different radii (leftmost column) polystyrene suspended in water and colloidal gold suspended in intralipid along with OCT reflectivity enhancement ratio (last column).

Radius (nm)	Maximum Backscattered intensity at 635.9 nm (a.u.)		Enhancement ratio of OCT reflectivity measured at 1310 nm
	Polystyrene particle in water	Gold nanoparticle in lipid	
40	0.16	0.99	1.02
75	0.36	1.01	1.85
125	0.06	0.96	4.04
Intralipid	-	0.88	-

As can be seen from the 2-D OCT maps of the phantom two layered structures shown for different radii 40 nm, 75 nm and 125 nm of the colloidal particles on the left column of the Fig. 7, there is first a small reflection at the air - layer agarose interface at first and is followed by almost no reflection because of the almost homogeneous layer of the lipid on the agarose layer. Again at the border between agarose + lipid and agarose+lipid+colloidal gold, there is a strong reflection at the interface. As can be seen, within this layer there is inhomogeneity with the introduction of highly backscattering colloidal gold particles and this back reflections depend on the radii of the particles used. There is increase with increasing particle size and the strongest back reflection was observed for the particle size of radius 125 nm.

Not only there is increase in intensity but also light propagates deeper due to increase in scattering. Summary of the results of backscattering enhancement from gold in agarose and lipid is given again in Table 1. A clear increase with respect to the particle size could be clearly seen with the largest increase seen for 125nm which is the best nearest appropriate size. Actually it should be mentioned here, that there were some difficulties with respect to consistency of the quality sample preparation. In spite of that we could fairly see a consistent increase for the case of 125nm.

4 Summary and Conclusions

We proposed a method for enhancing the reflectivity of optical coherence tomography signals through introduction of an appropriate sized nano metal particles into the sample under study. We chose gold nano particles due to their wide usage and availability in various sizes. The best size of the gold nano particles at a chosen wavelength and surrounding medium index can be determined based on Mie scattering theory. We could confirm the Mie-calculation results of increase in backscattering through basic scattering experiments.

For OCT experiment, we conducted phantom experiments with gold particles suspended in agarose mixed with intra-lipid. We could clearly see an enhancement in OCT reflectivity by a factor of 4 at a wavelength of 1310 nm and for a gold nano particle radius of 125 nm. We believe, we could largely incorporate these results in the functional OCT applications *in vivo* that are on going in our laboratory.

References

1. Huang D, Swanson E A, Lin C P, Schuman S, Stinson W G, Chang W, Hee M R, Flotte T, Gregory K, Puliafito C A, Fujimoto J G, *Science*, 254(1991)1178-1181.
2. Wojtkowski M, *Appl Opt*, 49(2010)D30-D61.
3. Drexler W, Fujimoto J G (eds), *Optical Coherence Tomography*, (Springer-Verlag), 2008.
4. Bouma B E, Tearney G J (eds), *Handbook of Optical Coherence Tomography*, (Marcel Dekker), 2002.
5. Rajagopalan Uma Maheswari, Takaoka H, Homma R, Tanifuji M, *J Neurosci Methods*, 124(2003)83-92.
6. Rajagopalan Uma Maheswari, Tanifuji M, *Opt Lett*, 32(2007)2614-2616.
7. Hyder F (ed), *Methods in Molecular biology: Dynamic Brain Imaging*, (Human Press), 2009, pp.111-132.
8. Lazebnik M, Marks D L, Potgieter K, Gillette R, Boppart S A, *Opt Lett*, 28(2003)1218-1220.
9. Yao X.- C, Yamauchi Perry A, B, George J. S, *Appl Opt*, 44(2005)2019-2023.
10. Bizheva K, Pflug R, Hermann B, Povazay B, Sattmann H, Qiu P, Anger E, Reitsamer H, Popov S, Taylor J R, Unterhuber A, Ahnelt P, Drexler W, *Proc Natl Acad Sci, USA*, 103(2006)5066-5071.
11. Srinivasan V J, Wojtkowski M, Fujimoto J G, Duker J S, *Opt Lett*, 31(2006)2308-2310.
12. Bohren C F, Huffman D R, *Absorption and scattering of light by small particles*, (John Wiley & Sons, Inc), 1983.
13. Kerker M, *The scattering of light and other electromagnetic radiation*, (Academic Press, New York), 1969.
14. Ishimaru A, *Wave propagation and scattering in random media*, (IEEE Press, New York), 1978.
15. Born M, Wolf E, *Principles of Optics*, (Pergamon Press, Oxford), 1980.
16. Rajagopalan Uma Maheswari, Kadono H, Tanifuji M, *Optical coherence tomographic imaging system for investigating cortical functional organization of brain: a simulation study*, *Proc SPIE*, Vol 3749, (1999); doi.org/10.1117/12.354805.

[Received: 02.10.2018; revised recd: 01.11.2018; accepted: 25.11.2018]



Manabu Tanifuji graduated from Osaka University, School of Engineering Science, and then studied at Osaka University where he received Doctor of Engineering in 1987. During his Ph D course, he investigated biophysics of ion channels by recording single channel events from ion channels incorporated in planar lipid bilayer membrane. After the course, he was appointed Assistant Professor at National Institute of Physiological Sciences, and then Associate Professor at Fukui University, Department of Information Science. At these institutions, he investigated signal propagation in visual cortical slices with voltage sensitive dye imaging.

In 1996, he moved to RIKEN, and currently is a Lab. Head of RIKEN Center for Brain Science where he investigates neural mechanisms of object recognition in macaque monkeys with physiological and optical recordings. Particularly, he revealed representation of object images and functional structures in macaque inferior temporal cortex, and he also invented a novel functional imaging technique (functional OCT) that enable us to resolve functional structures along the axis along light penetration